Transport of phosphatidylinositol 3-phosphate into the vacuole *via* autophagic membranes in *S. cerevisiae*

Keisuke Obara[1*], Takeshi Noda[2*], Kaori Niimi[1], and Yoshinori Ohsumi[1]

1 Department of Cell Biology, National Institute for Basic Biology, Okazaki 444-8585, Japan
2 Department of Cellular Regulation, Research Institute for Microbial Diseases, Osaka University, Osaka, Japan

*These authors contributed equally to this work

<Corresponding author>
Yoshinori Ohsumi
Department of Cell Biology, National Institute for basic biology, Okazaki 444-8585, Japan
Tel:+81+564-55-7515
Fax:+81-564-55-7516
E-mail:yohsumi@nibb.ac.jp

<Running Title>
Transport of PtdIns(3)*P* by autophagy

<Length of manuscript>
43893 characters

Abstract

Vps34, the sole PtdIns 3-kinase in yeast, is essential for autophagy. Here, we show that the lipid-kinase activity of Vps34 is required for autophagy, implying an essential role of its product PtdIns(3)*P*. The protein kinase activity of Vps15, a regulatory subunit of the PtdIns 3-kinase complex, is also required for efficient autophagy. We monitored the distribution of PtdIns(3)*P* in living cells using a specific indicator, the 2xFYVE domain derived from mammalian Hrs. PtdIns(3)*P* was abundant at endosomes and on the vacuolar membrane during logarithmic growth phase. Under starvation conditions, we observed massive transport of PtdIns(3)*P* into the vacuole. This accumulation was dependent on the membrane dynamics of autophagy. Notably, PtdIns(3)*P* was highly enriched and delivered into the vacuole as a component of autophagosome membranes but not as a cargo enclosed within them, implying direct involvement of this phosphoinositide in autophagosome formation. We also found a possible enrichment of PtdIns(3)*P* on the inner autophagosomal membrane compared to the outer membrane. Based on these results we discuss the function of PtdIns(3)*P* in autophagy.

Introduction

Eukaryotic cells are equipped with a self-digesting system called macroautophagy (hereafter, autophagy). Using this system, cells can degrade a portion of their cytoplasmic contents, sometimes including organelles, within a lytic compartment, the vacuole or lysosome. Autophagy is thought to be primarily a cell survival mechanism that enables recycling of macromolecules under nutrient starvation conditions. However, recent studies have shown that autophagy also plays roles in clearance of protein aggregate precursors, defense against invading pathogens, cell differentiation, and so on, highlighting the versatility of this system (Hara *et al*., 2006; Komatsu *et al*., 2006; Nakagawa *et al*., 2004). Electron microscopic analyses of starved yeast cells have shown that autophagy involves unique membrane dynamics, requiring *de novo* synthesis of double-membraned structures (Baba *et al*., 1994; Noda *et al*., 2002). Upon induction of autophagy, a cup-shaped isolation membrane emerges in the cytoplasm and elongates to enclose cytoplasmic contents. The isolation membrane fuses at its ends to become a closed double-membraned structure called the autophagosome. Autophagosomal membranes are thinner than other intracellular membranes (Baba et al., 1994). The lipid composition of autophagosomal membranes remains unknown since it is technically difficult to isolate autophagosomes with high purity. The autophagosome then fuses with a vacuole or lysosome, where the inner membrane structure is released into the lumen as an autophagic body and is degraded (Baba *et al*., 1994; Mizushima *et al*., 2001). This autophagosome formation step is a basic process in autophagy that occurs in a variety of situations.

The discovery of *ATG* (autophagy-related) genes opened a window for study of the molecular mechanisms underlying autophagosome formation (Tsukada *et al*., 1993; Thumm *et al*., 1994). Currently 31 *ATG* genes have been identified; among them, at least 18 are essential for normal autophagosome formation. These 18 genes are classified into 5 functional groups: (i) the protein kinase, Atg1, and associated proteins, (ii) phosphatidylinositol (PtdIns) 3-kinase complex, (iii) proteins involved in ubiquitin-like conjugation of Atg12 and Atg5, (iv) proteins involved in ubiquitin-like conjugation of Atg8 and phosphatidylethanolamine (PE), and (v) an Atg2, Atg18, and Atg9 protein complex of unknown function. Atg proteins partially localize to a peri-vacuolar structure called the pre-autophagosomal structure (PAS), the characteristics of which are still unclear (Suzuki *et al*., 2001). Several lines of pharmacological and molecular biological evidence have demonstrated that the two

ubiquitin-like conjugation systems and PtdIns 3-kinase are also essential for autophagy in mammalian and plant cells (Petiot *et al*., 2000; Mizushima *et al*., 2001; Yoshimoto *et al*., 2004). Most of the other *ATG* genes are also conserved in animals and plants, although whether they are essential for autophagy has not yet been clearly verified (Mizushima *et al*., 2002; Bassham *et al*., 2006).

Class III PtdIns 3-kinase (referred to as PtdIns 3-kinase herein) catalyzes phosphorylation of PtdIns, one of the major phospholipids in the cell, specifically at the D-3 position of the inositol ring, to generate PtdIns(3)*P*. Vps34, the sole PtdIns 3-kinase in yeast, is responsible for the production of PtdIns(3)*P* (Schu *et al*., 1993). Vps34 is required for membrane trafficking events including endocytosis, the sorting of soluble vacuolar proteins, multivesicular body formation, and autophagy (Munn and Riezman, 1994; Schu *et al*., 1993; Kihara *et al*., 2001; Katzmann *et al*., 2003). PtdIns(3)*P* is abundant on endosomal membranes (Burd and Emr, 1998; Gillooly *et al*., 2000), consistent with its involvement in trafficking events.

Vps34 forms different protein complexes that function exclusively in each process: PtdIns 3-kinase complex I functions in autophagy while complex II functions in vacuolar protein sorting (Kihara *et al*., 2001). Both of these complexes contain three common subunits, Vps15, Vps34, and Vps30/Atg6. Vps15 is a serine/threonine kinase that phosphorylates Vps34 to recruit it to the membrane (Stack *et al*., 1995). The protein-kinase activity of Vps15 is essential for complex formation, while the lipid-kinase activity of Vps34p is not (Kihara *et al*., 2001). While the function of Vps30 within these PtdIns 3-kinase complexes is not well understood, the homologous protein, Beclin 1, has been implicated in autophagy in both animals and plants (Liang *et al*., 1999; Liu *et al*., 2005). In addition to the common subunits, each complex also contains a unique factor. Atg14 is contained in complex I, while Vps38 is specific to complex II. These additional subunits may act as connecter molecules, bridging Vps30 and Vps34 to allow complex formation (Kihara *et al*., 2001). In addition, these specific subunits sort the function of PtdIns 3-kinase complexes by regulating their localization (Obara *et al*., 2006). Atg14 is required for the localization of complex I to the PAS, implying an important role in linking complex I to autophagy. Because *vps34*Δ cells have additional phenotypes beyond those of *vps30*Δ mutant cells (Robinson *et al*., 1988; Kihara *et al*., 2001), the Vps15-Vps34 complex or a novel complex (putative complex III) composed of Vps34, Vps15, and unknown subunit(s) is speculated to function in processes other than autophagy or vacuolar protein sorting.

How PtdIns 3-kinase complex I functions in autophagy is still poorly understood. While complex I shows PtdIns 3-kinase activity *in vitro*, *atg14*Δ cells exhibit a similar level of PtdIns 3-kinase activity to that in WT cells (Kihara *et al*., 2001). Thus, it remains unclear whether PtdIns 3-kinase complex I itself acts directly in autophagy in a kinase-independent manner, or whether the production of PtdIns(3)*P* is essential for autophagy.

In this study, we elucidate an essential role for PtdIns(3)*P* in autophagy. Monitoring of PtdIns(3)*P* showed dynamic movement of PtdIns(3)*P* into the vacuole under starvation conditions. We investigated the relationship between this transport and autophagic membrane dynamics, which implied direct involvement of PtdIns(3)*P* in autophagosome formation.

Results

Production of PtdIns(3)P and autophagy

Vps34, the sole PtdIns 3-kinase in the yeast, is essential for autophagosome formation (Kihara *et al*., 2001) and forms a complex with Vps15, Vps30/Atg6, and Atg14. However, there is little reduction in PtdIns 3-kinase activity in *ATG14* deletion mutant cells (Kihara *et al*., 2001). Therefore, it remains a question whether the Atg14-containing complex has roles in autophagy beyond PtdIns 3-kinase activity. To determine whether the lipid-kinase activity of Vps34 is required for autophagy, autophagic activity was estimated by accumulation of autophagic bodies in *vps34*Δ cells expressing vps34^{N736K} (Schu *et al*., 1993), a lipid kinase deficient form of Vps34. Cells expressing vps34^{N736K} did not accumulate autophagic bodies (Fig. 1), indicating that PtdIns 3-kinase activity and, in turn, its product, PtdIns(3)*P*, is essential for autophagy. Protein kinase activity of Vps15, the regulatory subunit of the PtdIns 3-kinase complex, was also essential for autophagy, as cells expressing vps15^{E200R}, a kinase deficient form of Vps15, did not accumulate autophagic bodies (Fig. 1). The Cvt (cytoplasm to vacuole targeting) pathway is not a degradative pathway, but is thought to be a type of selective autophagy in *S. cerevisiae* to deliver aminopeptidase I (Ape I) from the cytosol to the vacuole, where it matures. We therefore monitored the maturation of Ape I in these mutant cells. In cells expressing vps34^{N736K}, Ape I maturation was completely blocked, indicating that PtdIns(3)*P* plays an essential role in the Cvt pathway as well (Fig. 2). Ape I maturation was also defective in vps15^{E200R} cells, although some Ape I was processed upon starvation of these cells. This leaky phenotype most likely arises from the ability of vps15^{E200R} cells to produce small amounts of PtdIns(3)*P* (Stack *et al*., 1995). Conjugation of two ubiquitin-like molecules is essential for autophagy (Ohsumi, 2001): Atg12 is covalently conjugated to Atg5, and Atg8 is conjugated phosphatidylethanolamine (PE) (Mizushima *et al*., 1998; Kirisako *et al*., 2000; Ichimura *et al*., 2000). We examined whether these two conjugation reactions occur in cells deficient in production of PtdIns(3)*P*. The Atg12-Atg5 conjugate was formed in *vps34*Δ cells and *vps15*Δ cells (Fig. 2). Likewise, lipidation of Atg8 occurred in these mutants. Taken together, these data indicate that the lipid-kinase activity of Vps34 and product PtdIns(3)*P* are essential for autophagy but not for the enzymatic conjugation reactions. However, the cellular amount of Atg8-PE was larger in the PtdIns 3-kinase deficient mutant cells than that in WT cells (Fig. 2). We also observed that the efficiency of Atg8-PE formation was lower in these mutants. Thus, although PtdIns(3)*P* is not

essential for the conjugation reactions, it may regulate the efficiency of Atg8-PE formation indirectly (see discussion).

*Dynamics of PtdIns(3)*P

As we identified a critical role of PtdIns(3)*P* in autophagy, we next monitored the intracellular distribution of PtdIns(3)*P* in cells in logarithmic growth phase and under starvation conditions. We utilized the 2xFYVE domain of mammalian Hrs as a PtdIns(3)*P* sensor since it has been demonstrated to bind specifically to PtdIns(3)*P* with high affinity (Gillooly *et al*., 2000). EGFP or monomeric RFP (mRFP) was fused to the 2xFYVE domain and expressed in yeast cells. In growing cells, EGFP-2xFYVE signals were detected on punctate structures near the vacuole and on the vacuolar membrane (Fig. 3A) The peri-vacuolar punctate structures were mostly endosomes, as they were also labeled with Snf7-mRFP, an endosomal marker. Occasionally, other peri-vacuolar dots were observed (arrow in Fig. 3A); these signals represent PtdIns(3)*P* at the PAS, as they co-localized with Atg17, a PAS marker (data not shown). These patterns agree with the previously observed distribution of PtdIns 3-kinase complexes (Obara *et al*., 2006). In *vps34*Δ cells, the 2xFYVE domain fusions were dispersed in the cytoplasm, verifying the specific binding of these proteins to PtdIns(3)*P* (Fig. 3B).

After transferring cells to nitrogen-depleted medium, a dramatic change in the distribution of mRFP-2xFYVE was observed: the signals became prominent in the vacuolar lumen, and the signals on the vacuolar rims and endosomes decreased (Fig. 3C). This result implies active transport of PtdIns(3)*P* into the vacuole under nitrogen starvation. We assessed whether the transport of mRFP-2xFYVE into the vacuole was evoked by rapamycin treatment, which mimics nitrogen starvation. In rapamycin-treated cells, a majority of the mRFP-2xFYVE signal was observed in the lumen of the vacuoles (Fig. 3C). These observations suggest that transport of PtdIns(3)*P* into the vacuole is triggered in response to starvation signals. Although the mRFP-2xFYVE signal at the vacuolar rim and peri-vacuolar area became less prominent or totally disappeared following starvation, this does not necessarily mean that PtdIns(3)*P* levels were diminished in these sites because the amount of the mRFP-2xFYVE sensor is limiting within each cell and its transport into the vacuole is irreversible.

*Transport of PtdIns(3)*P *into the vacuole* via *autophagy*

Since both nitrogen starvation and rapamycin treatment induce autophagy, we assessed whether autophagy is responsible for the transport of PtdIns(3)*P* into the vacuole. Autophagy-deficient *atg14*Δ cells were not able to transport mRFP-2xFYVE into the vacuole; in contrast, in *vps38*Δ cells, which have normal autophagy but are defective for sorting of vacuolar hydrolases, mRFP-2xFYVE was transported into the vacuole normally. Disruption of the *ATG14* gene in Δ*vps38* cells abrogated the transport of mRFP-2xFYVE into the vacuole. Cells lacking Vps30/Atg6, a common subunit of PtdIns 3-kinase complexes I and II, and required for both autophagy and sorting, were also defective for transport of mRFP-2xFYVE into the vacuole. Thus, production of PtdIns(3)*P* by PtdIns 3-kinase complex I is responsible for the delivery of PtdIns(3)*P* into the vacuole lumen. Given that the generation of Atg12-Atg5 and Atg8-PE by the Atg7 E1 enzyme was unaffected in the absence of PtdIns(3)*P* (Fig. 2) and the localization of Atg14 is normal in *atg7*Δ cells (Suzuki *et al*., 2001), it seems likely that autophagy associated PtdIns(3)*P* is generated in *atg7Δ* cells. Nevertheless, the appearance of mRFP-2xFYVE signal in the vacuolar lumen was not prominent in these cells, in striking contrast to WT cells (Fig. 4A). These results indicate that autophagic membrane flow itself is involved in the transport of mRFP-2xFYVE into the vacuole under starvation conditions. The autophagy-dependent transport of mRFP-2xFYVE into the vacuole was further confirmed biochemically. After transportation into the vacuole, mRFP-2xFYVE should be cleaved at the linker sequence between mRFP and 2xFYVE, as seen in the case of ApeI-GFP (Suzuki *et al*., 2002). The resultant mRFP moiety can be detected by immunoblot analysis with an anti-DsRed antibody. The full-length mRFP-2xFYVE outside the vacuole can be detected with an affinity-purified anti-FYVE antibody. In association with the progression of autophagy, the amount of released mRFP moiety increased in WT and *vps38*Δ cells (Fig. 4B), while the amount of mRFP-2xFYVE decreased. Autophagy-deficient *atg14*Δ cells contained a basal level of mRFP, which did not increase under starvation conditions. A substantial amount of mRFP-2xFYVE remained under starvation conditions in *atg14*Δ cells. These results are in good agreement with the microscopic analysis. Phenylmethylsulfonyl fluoride (PMSF), a serine protease inhibitor, inhibits breakdown of the cytoplasmic contents delivered to the vacuole *via* autophagy without affecting autophagosome formation (Takeshige *et al*., 1992). The cleavage of mRFP-2xFYVE was blocked by addition of PMSF and the level of mRFP-2xFYVE was maintained in starved WT and *vps38*Δ cells (Fig. 4C). Thus, we confirmed that mRFP-2xFYVE is transported into the vacuole *via* autophagy and degraded inside the vacuole.

These microscopic and biochemical analyses highlight a the transport of PtdIns(3)*P* into the vacuole *via* autophagy.

To investigate how autophagy is involved in this process, autophagic bodies were allowed to accumulate within the vacuole following addition of PMSF to the starvation medium. After 4 h of nitrogen starvation, a number of structures were observed to move within the vacuole. mRFP-2xFYVE signals were detected on these structures. Using the simultaneous excitation and detection system (see Experimental procedures), these structures were shown to co-localize with GFP-Atg8, a marker for autophagosomes and resultant autophagic bodies (Kirisako *et al*., 1999) (Fig. 5A). Serial observation showed that the GFP-Atg8 and mRFP-2xFYVE signals within the vacuole moved together (see movie in Fig. S1), indicating that mRFP-2xFYVE is transported into the vacuole *via* autophagosomes.

Under nitrogen starvation conditions, yeast cells generate relatively uniform autophagosomes/autophagic bodies that are approximately 500 to 600 nm in diameter. They are not large enough to distinguish between the membrane of the autophagic body (which corresponds to the inner membrane of the autophagosome) and its lumen (corresponding to the enclosed cargo) using fluorescence microscopy. To investigate whether PtdIns(3)*P* is enriched in the membranes of autophagic bodies or is enclosed within their lumens, autophagy was induced in medium depleted of both nitrogen and carbon sources. Cells cultured in this medium accumulate relatively large autophagic bodies that sometimes reach 800 to 900 nm in diameter. Some cells cultured in this medium accumulated large autophagic bodies that were intensely labeled at their rims, displaying ring-shaped fluorescence (Fig. 5B; see movie in Fig. S2). A ring-shaped structure labeled with mRFP-2xFYVE was also seen at the peri-vacuolar site (arrow in Fig. 5B), probably representing an autophagosome prior to fusion with the vacuole or an isolation membrane prior to enclosure. These observations strongly suggest that PtdIns(3)*P* is enriched at autophagosomes and transported into the vacuole as a component of the membrane rather than as enclosed cargo. The fact that negligible mRFP-2xFYVE signal was dispersed in the cytosol supports this idea. To provide further support, mRFP-2xFYVE fusion protein was detected by immunoelectron microscopy with affinity-purified anti-FYVE antibody. Gold particles were detected primarily on the membranes of isolation membranes, autophagosomes and autophagic bodies (Fig. 5C). These signals are highly specific to mRFP-2xFYVE since almost no signal was obtained in negative control cells that do not express mRFP-2xFYVE despite normal occurrence of autophagy (data not shown). Based on the corroborating results of these assays, we conclude that

PtdIns(3)*P* is enriched at autophagosome membranes and is transported into the vacuole under starvation conditions. Interestingly, the inner surface of isolation membranes and autophagosomes were preferentially labeled compared to the outer membranes (Fig. 5C). We also occasionally observed signals beside the tips of elongating isolation membranes (arrowheads in Fig. 5C).

Discussion

In this work, we have shown an essential role of PtdIns 3-kinase activity and its product PtdIns(3)*P* in autophagy. Monitoring of PtdIns(3)*P* demonstrated autophagy-dependent transport of this phosphoinositide into the vacuole under starvation conditions. PtdIns(3)*P* is delivered to the vacuole via enrichment on autophagosome and autophagic body membranes, rather than as a cargo enclosed within them; this implies an important and direct role of PtdIns(3)*P* in autophagosome formation.

In a previous study, a role of PtdIns(3)*P* in the initiation of autophagosome formation was suggested because PAS localization of several Atg proteins was disturbed in *atg14*Δ mutant cells. However, a role of PtdIns(3)*P* during elongation of the membrane has not been discussed. One important finding herein is that PtdIns(3)*P* is localized not only at the PAS, as expected from the localization of Atg14, but also on autophagosomal membranes. To date, the lipid composition of autophagosomal membranes has been totally unknown except that PE is supposed to be present as Atg8-PE localize onto autophagosomal membranes (Kirisako et al., 1999). Thus, our finding that PtdIns(3)*P* is highly enriched on autophagosomal membranes provides important basic information to gain insights into the nature and the formation mechanism of this mysterious double membrane structure.

Since the autophagic body membrane corresponds to the inner autophagosome membrane, high levels of PtdIns(3)*P* on the autophagic body membrane reflects enrichment on the inner autophagosome membrane, which was supported by electron microscopic analysis (Fig. 5C). In contrast, we observed much less PtdIns(3)*P* on the outer surface of autophagosome membranes. Several possibilities may explain this result: i) PtdIns(3)*P* may not be produced on the outer membrane, ii) PtdIns(3)*P* on the outer membrane may be metabolized by a lipid phosphatase, or iii) PtdIns(3)*P*-enriched membranes may be supplied preferentially to the inner membrane. However, we do not thoroughly exclude the possibility that PtdIns(3)*P* on the outer membrane may be difficult to detect due to experimental limitations, *e.g.* coat proteins on the outer membrane may make it difficult for mRFP-2xFYVE to bind PtdIns(3)*P*. We also occasionally observed the enrichment of PtdIns(3)*P* next to the elongating tips of isolation membranes (Fig. 5C). It is an intriguing speculation that such PtdIns(3)*P*-enriched unknown structures are supplying lipids to the isolation membranes. Alternatively, it would be also an interesting future issue to investigate the relationship between these PtdIns(3)*P*-positive ambiguous structures and the PAS which has not been visualized successfully by electron microscopy. We are studying on these topics,

which will provide further insight into the role of PtdIns(3)*P* in autophagosome formation.

How is enrichment of PtdIns(3)*P* involved in autophagosome formation? It is possible that PtdIns(3)*P* directly affects the curvature of the isolation membrane without assistance of PtdIns(3)*P*-binding effectors. Although we do not thoroughly exclude this possibility, we prefer an alternative hypothesis that enrichment of PtdIns(3)*P* assists PtdIns(3)*P*-binding molecules to concentrate on the isolation membrane. To date, Atg18, Atg21, Atg20, and Atg24 have been shown to bind to PtdIns(3)*P* by *in vitro* PIP strip assays, although these results should be further verified by other methods (Nice *et al*., 2002; Krick *et al*., 2006; Michell *et al*., 2006). In addition, microscopy has shown that Atg14 is required for the PAS localization of Atg2, Atg8, Atg16, and Atg12-Atg5 conjugate (Shintani *et al*., 2001; Suzuki *et al*., 2007). These proteins are candidate downstream effectors of PtdIns(3)*P*. It is difficult to distinguish the PAS and isolation membrane/autophagosome using fluorescence microscopy in yeast cells because the autophagosomes are not large enough. Cup-shaped isolation membranes, as seen in Fig. 5, are not always identified. Therefore, it is still unclear whether these possible effectors are recruited by PtdIns(3)*P* directly onto the elongating isolation membrane or to the PAS prior to the onset of membrane formation. Recently, Nakatogawa *et al*. (2007) showed that Atg8-PE has an activity that mediates tethering and hemifusion of membranes, which implies direct involvement of Atg8-PE in generating isolation membranes. In mammalian cells, Atg12-Atg5 together with Atg16 is proposed to function on elongating isolation membranes (Mizushima *et al*., 2001). These reports suggest that these putative PtdIns(3)*P* effectors participate in the membrane formation process rather than in regulation of autophagy. In contrast, localization of Atg17 and Atg11, which are thought to be PAS scaffold proteins, is not affected in *atg14*Δ cells (Suzuki *et al*., 2007). Taken together, we speculate that PtdIns(3)*P* produced by complex I spatially coordinates the scaffold proteins and the molecules that are directly involved in membrane formation.

The steady-state level of Atg8 was higher in PtdIns 3-kinase deficient mutant cells compared to WT cells. This is probably a secondary effect due to the blockage of the Cvt pathway and autophagy, and to the elevated expression of Atg8 caused by the cellular stress in these mutant cells lacking PtdIns(3)*P*. In addition, the efficiency of Atg8 lipidation appeared to be lower in these mutants. Recent studies showed that the Atg12-Atg5 conjugate has an E3-like activity in Atg8-PE formation (Hanada et al., 2007; Fujita et al., 2008). Given that the localization of Atg12-Atg5 conjugate and Atg8 is affected in *atg14*Δ cells (Suzuki et al.,

2007), it is likely that PtdIns(3)*P* regulates the efficiency of Atg8-PE formation through the localization of the Atg12-Atg5 conjugate and/or Atg8 itself.

Monitoring of PtdIns(3)*P* also provided other information. During logarithmic phase, a majority of PtdIns(3)*P* was located at endosomes and vacuolar membranes. Only a minor population of cells contained PtdIns(3)*P* at the PAS. The Cvt pathway is active under these conditions at the PAS (Suzuki *et al*., 2002). The small number of cells exhibiting 2xFYVE signals at the PAS may suggest that PtdIns(3)*P* is transiently produced at the PAS and rapidly utilized by the Cvt pathway. It was previously shown that PtdIns(3)*P* is transported into the vacuolar lumen *via* the multivesicular body pathway under non-starved conditions (Wurmser and Emr, 1998). These two pathways are thought to be responsible for PtdIns(3)*P* transport into the vacuole under nutrient-rich conditions. However, the extent of PtdIns(3)*P* transport into the vacuole by these pathways was much smaller than that by autophagy under starvation conditions (Figs. 3 and 4). We detected substantial 2xFYVE signal on both vacuolar and endosomal membranes (Fig. 3). This pattern is consistent with the localization of PtdIns 3-kinase complexes (Obara *et al*., 2006). We also showed that cells lacking both Atg14 and Vps38 still exhibit 2xFYVE signals at peri-vacuolar punctate structures and the vacuolar membrane (Fig. 4). These punctate structures are endosomes, as they co-localized with Snf7-mRFP, an endosomal marker protein (our unpublished results). In *vps38*Δ and *atg14*Δ*vps38*Δ cells, endosomal localization of Vps30 is lost, which indicates that the PtdIns 3-kinase complex II localizes to endosomes in a Vps38-dependent manner (Obara *et al*., 2006). However, in these cells, some portion of Vps15 and Vps34 still localize to peri-vacuolar punctate structures and the vacuolar membrane. These likely represent Vps34-Vps15 complex or an undefined PtdIns 3-kinase complex (complex III) containing Vps15, Vps34, and unknown subunit(s) other than Vps30 (Obara *et al*., 2006). The Vps34- and Vps15-positive punctate structures were labeled with Snf7-mRFP (our unpublished results). Thus, the residual PtdIns(3)*P* at the endosome and the vacuolar membrane in *atg14*Δ*vps38*Δ cells is likely to be produced by Vps15-Vps34 complex or a putative PtdIns 3-kinase complex III remaining at these sites.

Experimental procedures

Yeast strains and media

The *Saccharomyces cerevisiae* strains used in this study were derived from SEY6210 (Robinson *et al*., 1988) or BJ2168 (yeast genetic center), as specified in Table 1. We used standard methods and media for yeast manipulation (Kaiser *et al*., 1994). Autophagy was induced by transferring the cells into nitrogen-depleted medium SD (-N), or nitrogen- and carbon-depleted medium S (-NC). Rapamycin was directly added to the medium at a final concentration of 0.2 μg/ml. PMSF was added directly to the medium at the onset of starvation at a final concentration of 1 mM.

Genetic and DNA manipulations

Gene disruption was performed by replacing the entire or part of the coding region with a marker gene. Successful gene disruption was verified by PCR and immunoblot analysis. The *SNF7-mRFP* strain was generated as follows. The sequence encoding mRFP (monomeric RFP; Campbell *et al*., 2002*)* was amplified by PCR from the *mRFP* sequence on pRSETB vector obtained from the Carlsberg Research Center, such that *Pac* I and *Asc* I sites were generated at the 5' and 3' ends, respectively. The amplified fragment was ligated into *Pac* I/*Asc* I digested pFA6a-GFP (S65T)-kanMX6 to replace the GFP sequence. The region containing *mRFP*, the *ADH1* termination sequence, and the *kanMX6* marker was amplified by PCR with a primer set containing the homologous region of the target gene. Amplified cassettes were inserted directly into the chromosome. Successful tagging of mRFP to the C-terminus of Snf7 was verified by PCR analysis and fluorescence microscopy.

Plasmids for the expression of Vps34 (pKHR54), vps34^{N736K} (pKHR60), Vps15 (pKHR55), and vps15^{E220R} (pKHR59) in yeast cells are described in Kihara *et al*. (2001). The plasmid for the expression of EGFP-2xFYVE in yeast cells (pOK104) was generated as follows. An *Nhe* I/*Sal* I fragment covering the *EGFP-2xFYVE* sequence was excised from pEGFP-2xFYVE (kind gift from Dr. H. Stenmark) and ligated into *Xba* I/*Sal* I digested p416TEF (Mumberg *et al*., 1995). The plasmid for the expression of mRFP-2xFYVE in yeast cells (pOK107) was generated as follows. The sequence encoding mRFP was amplified by PCR such that *Xba* I and *Hind* III sites were generated at the 5' and 3' ends, respectively. A *Hind* III/*Sal* I fragment covering the *2xFYVE* sequence was excised from pEGFP-2xFYVE. These two fragments were ligated together into *Xba* I/*Sal* I digested p416TEF to generate the

mRFP-2xFYVE sequence in p416TEF. Successful construction of the plasmid was verified by sequencing. Expression of these fusion proteins did not affect autophagy, as verified by normal accumulation of autophagic bodies (see Fig. 5).

Microscopy

The intracellular localization of GFP- and mRFP-tagged proteins was observed using inverted fluorescence microscopes (IX-71 and IX-81, Olympus) equipped with cooled CCD cameras (CoolSNAP HQ, NIPPON ROPER). For the simultaneous observation of EGFP- and mRFP-fusion proteins, cells were excited simultaneously with blue (Sapphire 488-20, Coherent) and yellow lasers (85-YCA-010, Melles Griot). A U-MNIBA2, from which the excitation filter was removed, was used for GFP visualization, and an FF593-Di02 dichroic mirror and an FF593-Em02 excitation filter (Semrock) were used to analyze mRFP. The accumulation of autophagic bodies was examined by phase-contrast microscopy. Images were acquired using MetaMorph software (UNIVERSAL IMAGING) and processed using Adobe PhotoShop software (Adobe).

Immunoelectron microscopy

Yeast cells expressing mRFP-2xFYVE were transferred to SD (-N) medium and collected after 3.5 h. Cells were processed using immunoelectron microscopy techniques as reported previously (Baba *et al*., 1994) with affinity-purified anti-FYVE antibody.

Immunoblotting

Immunoblotting was performed using anti-ApeI (kind gift from Dr. D. Klionsky), anti-Atg12, anti-Atg8 (Kirisako *et al*., 2000), anti-DsRed (kind gift from Dr. T. Endo), affinity-purified anti-FYVE domain of mamamalian Hrs, and affinity-purified anti-Vps34 (Kihara *et al*., 2001) antibodies. Immunodetection utilized an ECL system (Amersham Biosciences) with a bioimaging analyzer (LAS1000, Fujifilm). Separating gels containing 6M urea were used to separate lipidated and unconjugated Atg8 (Kirisako *et al*., 2000).

Acknowledgements

We thank Dr. Harald Stenmark, Dr. Roger Y. Tsien, Dr. Daniel J. Klionsky, and Dr. Toshiya Endo for providing the 2xFYVE domain plasmids, mRFP plasmid, anti-ApeI antibody, and anti-DsRed antibody, respectively. We also thank Ms. Ichikawa and the NIBB Center for Analytical Instruments for their technical support. This work was supported in part by Grants-in-Aids for Scientific Research from the Ministry of Education, Culture, Sports, Science and Technology of Japan.

References

Baba, M., Takeshige, K., Baba, N., and Ohsumi, Y. (1994). Ultrastructural analysis of the autophagic process in yeast: detection of autophagosomes and their characterization. *J. Cell Biol*. 124:903-913

Bassham, D.C., Laporte, M., Marty, F., Moriyasu, Y., Ohsumi, Y., Olsen, L.J., and Yoshimoto, K. (2006) Autophagy in development and stress responses of plants. *Autophagy* 2: 2-11

Burd, C.G. and Emr, S.D. (1998) Phosphatidylinositol(3)-phosphate signaling mediated by specific binding to RING FYVE domains. *Mol. Cell* 2: 157-162

Campbell, R.E., Tour, O., Palmer, A.E., Steinbach, P.A., Baird, G.S., Zacharias, D.A., and Tsien, R.Y. (2002) A monomeric red fluorescent protein. *Proc. Natl. Acad. Sci. USA*. 99:7877-7882

Fujita, N., Itoh, T., Fukuda, M., Noda, T., and Yoshimori, T. (2008) The Atg16L complex specifies the site of LC3 lipidation for membrane biogenesis in autophagy. *Mol. Biol. Cell* in press.

Gillooly, D.J., Morrow, I.C., Lindsay, M., Gould, R., Bryant, N.J., Gaullier, J.M., Parton, R.G., and Stenmark H. (2000) Localization of phosphatidylinositol 3-phosphate in yeast and mammalian cells. *EMBO J*. 19:4577-4588

Hanada, T., Noda, N.N., Satomi, Y., Ichimura, Y., Fujioka, Y., Takao, T., Inagaki, F., and Ohsumi, Y. (2007) The Atg12-Atg5 conjugate has a novel E3-like activity for protein lipidation in autophagy. *J. Biol. Chem* 282: 37298-37302

Hara, T., Nakamura, K., Matsui, M., Yamamoto, A., Nakahara, Y., Suzuki-Migishima, R. Yokoyama, M., Mishima, K., Saito, I., Okano, H., and Mizushima, N. (2006) Suppression of basal autophagy in neural cells causes neurodegenerative disease in mice. *Nature* 441: 885-889

Ichimura, Y., Kirisako, T., Takao, T., Satomi, Y., Shimonishi, Y., Ishihara, N., Mizushima, N., Tanida, I., Kominami, E., Ohsumi, M., Noda, T. and Ohsumi, Y. (2000) A ubiquitin-like system mediates protein lipidation. *Nature* 408:488-492

Kaiser, C., Michaelis, S., and Mitchell, A. (1994). Methods in Yeast Genetics, Cold Spring Harbor, NY: Cold Spring Harbor Laboratory Press.

Katzmann, D.J., Stefan, C.J., Babst, M., and Emr, S.D. (2003) Vps27 recruits ESCRT machinery to endosomes during MVB sorting. *J. Cell Biol*. 162:413-423

Kihara, A., T. Noda, N. Ishihara, and Y. Ohsumi. (2001). Two distinct Vps34 phosphatidylinositol 3-kinase complexes function in autophagy and carboxypeptidase Y sorting in *Saccharomyces cerevisiae*. *J. Cell Biol*. 152:519–530.

Kirisako, T., Baba, M., Ishihara, N., Miyazawa, K., Ohsumi, M., Yoshimori, T., Noda, T., and Ohsumi, Y. (1999). Formation process of autophagosome is traced with Apg8/Aut7p in yeast. *J. Cell Biol*. 147:435-446

Kirisako, T., Ichimura, Y., Okada, H., Kabeya, Y., Mizushima, N., Yoshimori, T., Ohsumi, M., Noda, T. and Ohsumi, Y. (2000) Reversible modification regulates the membrane-binding state of Apg8/Aut7 essential for autophagy and the cytoplasm to vacuole targeting pathway. *J. Cell Biol* 151: 263-276

Komatsu, M., Waguri, S., Chiba, T., Murata, S., Iwata, J., Tanida, I., Ueno, T., Koike, M., Uchiyama, Y., and Kominami, E., Tanaka, K. (2006) Loss of autophagy in the central nervous system causes neurodegeneration in mice. *Nature* 441: 880-884.

Krick, R., Tolstrup, J., Appelles, A., Henke, S., and Thumm, M. (2006) The relevance of the phosphatidylinositolphosphat-binding motif FRRGT of Atg18 and Atg21 for the Cvt pathway and autophagy. *FEBS Lett*. 580:4632-4638

Liang, X.H., Jackson, S., Seaman, M., Brown, K., Kempkes, B., Hibshoosh, H., and Levine, B. (1999). Induction of autophagy and inhibition of tumorigenesis by *beclin 1*. *Nature* 402:

672-676

Liu, Y., Schiff, M., Czymmek, K., Talloczy, Z., Levine, B., and Dinesh-Kumar, S.P. (2005). Autophagy regulates programmed cell death during the plant innate immune response. *Cell* 121:567-577.

Michell, R.H., Heath, V.L., Lemmon, M.A., and Dove, S.K.(2006) Phosphatidylinositol 3,5-bisphosphate: metabolism and cellular functions. *Trends Biochem. Sci.* 3: 52-63

Mizushima, N., Noda, T., Yoshimori, T., Tanaka, Y., Ishii, T., George, M.D., Klionsky, D.J., Ohsumi, M., and Ohsumi, Y. (1998) A protein conjugation system essential for autophagy. *Nature* 395:395-398

Mizushima, N., Yamamoto, A., Hatano, M., Kobayashi, Y., Kabeya, Y., Suzuki, K., Tokuhisa, T., Ohsumi, Y. and Yoshimori, T. (2001) Dissection of autophagosome formation using Apg5-deficient mouse embryonic stem cells. *J. Cell Biol.* 152: 657-667

Mizushima, N., Ohsumi, Y., and Yoshimori, T. (2002) Autohpagosome formation in mammalian cells. *Cell Struct. Funct.* 27: 421-429

Mumberg, D., Muller, R., and Funk, M. (1995) Yeast vectors for the controlled expression of heterologous proteins in different genetic backgrounds. *Gene* 156:119-122

Munn, A.L., and Riezman, H. (1994) Endocytosis is required for the growth of vacuolar H(+)-ATPase-defective yeast: identification of six new *END* genes. *J. Cell Biol.* 127: 373-386

Nakagawa, I., Amano, A., Mizushima, N., Yamamoto, A., Yamaguchi, H., Kamimoto, T., Nara, A., Funao, J., Nakata, M., Tsuda, K., Hamada, S., and Yoshimori, T. (2004) Autophagy defenses cells against invading group A Streptococcus. *Science* 306: 1037-1040

Nakatogawa, H., Ichimura, Y., and Ohsumi, Y. (2007) Atg8, a ubiquitin-like protein required for autophagosome formation, mediates membrane tethering and hemifusion. *Cell* 130:165-178

Nice, D.C., Sato, T.K., Stromhaug, P.E., Emr, S.D., and Klionsky, D.J. (2002) Cooperative binding of the cytoplasm to vacuole targeting pathway proteins, Cvt13 and Cvt20, to phosphatidylinositol 3-phosphate at the pre-autophagosomal structure is required for selective autophagy. *J. Biol. Chem.* 277:30198-30207

Noda, T., Suzuki, K., and Ohsumi, Y. (2002). Yeast autophagosomes: de novo formation of a membrane structure. *Trends Cell Biol.* 12: 231-235

Obara, K., Sekito, T., and Ohsumi, Y. (2006) Assortment of phosphatidylinositol 3-kinase complexes - Atg14p directs association of complex I to the pre-autophagosomal structure in *S. cerevisiae* -. *Mol. Biol. Cell* 17, 1527-1539.

Ohsumi, Y. (2001) Molecular dissection of autophagy: two ubiquitin-like systems. *Nat. Rev. Mol. Cell Biol.* 2: 211-216

Petiot, A., Ogier-Denis, E., Blommaart, E.F., Meijer, A.J., and Codogno, P. (2000). Distinct classes of phosphatidylinositol 3'-kinases are involved in signaling pathways that control macroautophagy in HT-29 cells. *J. Biol. Chem.* 275:992-998

Robinson, J.S., Klionsky, D.J., Banta. L.M., and Emr, S.D. (1988). Protein sorting in *Saccharomyces cerevisiae*: isolation of mutants defective in the delivery and processing of multiple vacuolar hydrolases. *Mol. Cell Biol.* 8:4936-4948

Schu, P.V., Takegawa, K., Fry, M.J., Stack, J.H., Waterfield, M.D., and Emr, S.D. (1993). Phosphatidylinositol 3–kinase encoded by yeast *VPS34* gene essential for protein sorting. *Science* 260:88-91

Shintani, T., Suzuki, K., Kamada, Y., Noda, T., Ohsumi, Y. (2001). Apg2p functions in autophagosome formation on the perivacuolar structure. *J. Biol. Chem.* 276:30452-30460

Stack, J.H., DeWald, D.B., Takegawa, K., and Emr, S.D. (1995). Vesicle-mediated protein transport: regulatory interactions between the Vps15 protein kinase and the Vps34 PtdIns

3–kinase essential for protein sorting to the vacuole in yeast. *J. Cell Biol*. 129:321-334

Suzuki, K., Kamada, Y., and Ohsumi, Y. (2002) Studies of cargo delivery to the vacuole mediated by autophagosomes in *Saccharomyces cerevisiae*. *Dev. Cell* 3:815-824

Suzuki, K., Kirisako, T., Kamada, Y., Mizushima, N., Noda. T., and Ohsumi, Y. (2001). The pre-autophagosomal structure organized by concerted functions of *APG* genes is essential for autophagosome formation. *EMBO J*. 20:5971-5981

Suzuki, K., Kubota, Y., Sekito, T., and Ohsumi, Y. (2007) Hierarchy of Atg proteins in pre-autophagsomal structure organization. *Genes Cells* 12: 209-218.

Takeshige, K., Baba, M., Tsuboi, S., Noda, T., and Ohsumi, Y. (1992) Autophagy in yeast demonstrated with proteinase-deficient mutants and conditions for its induction. *J. Cell Biol*. 119:301-311

Thumm, M., Egner, R., Koch, B., Schlumpberger, M., Straub, M., Veenhuis, M., and Wolf, D.H. (1994). Isolation of autophagocytosis mutants of *Saccharomyces cerevisiae*. *FEBS Lett*. 349: 275-280.

Tsukada, M., and Ohsumi, Y. (1993) Isolation and characterization of autophagy-defective mutants of *Saccharomyces cerevisiae*. *FEBS Lett*. 333:169-174.

Wurmser, A.E., and Emr, S.D. (1998) Phosphoinositide signaling and turnover: PtdIns(3)P, a regulator of membrane traffic, is transported to the vacuole and degraded by a process that requires lumenal vacuolar hydrolase activities. *EMBO J*. 17:4930-4942.

Yoshimoto, K., Hanaoka, H., Sato, S., Kato, T., Tabata, S., Noda, T., and Ohsumi, Y. (2004) Processing of ATG8s, ubiquitin-like proteins, and their deconjugation by ATG4s are essential for plant autophagy. *Plant Cell* 16: 2967-2983.

Figure legends

Figure 1 PtdIns 3-kinase activity is essential for autophagy.

Cells cultured in S (-NC) medium containing 1 mM PMSF for 4 h were observed by phase contrast microscopy. Autophagic bodies accumulated in the vacuole are indicated by arrows. Bar, 5 μm.

Figure 2 PtdIns 3-kinase activity is essential for the Cvt pathway.

Cells at logarithmic phase (starvation -) were transferred to SD (-N) medium and cultured for 4 h (starvation +). Lysates were prepared by the alkaline-TCA method and subjected to immunoblot analysis.

Figure 3 PtdIns(3)*P* is transported into the vacuole under starvation conditions.

A, cells at logarithmic phase were subjected to microscopy. EGFP-2xFYVE and Snf7-mRFP were simultaneously excited and their fluorescence was acquired concomitantly (see Experimental Procedures). EGFP-2xFYVE signals co-localized with Snf7-mRFP signals are indicated by arrowheads. Arrow indicates an EGFP-2xFYVE signal that was not co-localized with Snf7-mRFP. B, WT and *vps34*Δ cells at logarithmic phase were subjected to microscopy. C, cells at logarithmic phase (0 h), 4 h following rapamycin treatment, or cultured in SD (-N) medium for the indicated time were observed by fluorescence microscopy. Bars, 5 μm.

Figure 4 PtdIns(3)*P* is transported into the vacuole *via* autophagy.

A, cells cultured in SD (-N) medium for 4 h were subjected to microscopy. Bar, 5 μm. B, Lysates prepared from cells at logarithmic phase (0 h), and cells cultured in SD (-N) medium for the indicated time were subjected to immunoblot analysis. C, Lysates prepared from cells at logarithmic phase (0 h), and cells cultured in SD (-N) medium for the indicated time with or without 1 mM PMSF were subjected to immunoblot analysis. Asterisk indicates a non-specific band.

Figure 5 PtdIns(3)*P* is enriched on autophagosomal and autophagic body membranes.

A, Cells cultured in SD (-N) medium containing 1mM PMSF for 5 h were subjected to microscopy. GFP-Atg8 and mRFP-2xFYVE were simultaneously excited and their fluorescence was acquired concomitantly (also see the movie in Figure S1). Bar, 5 μm. B, WT cells were cultured in S (-NC) medium containing 1 mM PMSF for 4 h and subjected to

microscopy. Autophagic bodies labeled with mRFP-2xFYVE at their rims are indicated by arrowheads (also see the movie in Figure S2). An elongating isolation membrane or closed autophagosome outside the vacuole is indicated by the arrow. The outline of the vacuole is indicated by a dotted line. Bars, 5 μm. C, BJ2168 cells expressing mRFP-2xFYVE were cultured in SD (-N) medium for 3.5 h and subjected to immunoelectron microscopy with affinity-purified anti-FYVE antibody. Gold particles on the inner membrane (IM) of the isolation membrane (ISM in a and c), autophagosome (AP in c and d), and on autophagic body (AB in b) membranes were indicated by arrows. Ribosomes appear more hazy than gold particles, and can therefore be distinguished. OM, outer membrane. V, vacuole. Bars, 100 nm.

Figure S1 PtdIns(3)*P* is enriched on autophagic bodies.
Cells expressing GFP-Atg8 and mRFP-2xFYVE were cultured in SD (-N) medium containing 1mM PMSF for 5 h and subjected to microscopy. GFP-Atg8 and mRFP-2xFYVE were simultaneously excited and their fluorescence was acquired concomitantly. The movie was constructed from 20 serial images taken at 150 msec intervals. The GFP-Atg8 image (top left), mRFP-2xFYVE image (top right), and their merged image (bottom) are shown.

Figure S2 PtdIns(3)*P* is enriched on autophagosomal and autophagic body membranes.
WT cells expressing mRFP-2xFYVE were cultured in S (-NC) medium containing 1 mM PMSF for 4 h and subjected to microscopy. The movie was constructed from 20 serial images taken at 50 msec intervals.

Table 1. Strains used in this study

Strain	Genotype	Source
SEY6210	*MATα leu2-3,112 ura3-52 his3Δ200 trp1Δ901 lys2-801 suc2-Δ9*	Robinson *et al*., 1988
YOK161	SEY6210 *vps34*Δ::*TRP1*	This study
YOK212	SEY6210 *vps15*Δ::*TRP1*	This study
YOK481	SEY6210 *SNF7-mRFP:kanMX6*	This study
GYS115	SEY6210 *atg14*Δ::*LEU2*	Suzuki *et al*., 2001
YOK135	SEY6210 *vps38*Δ::*HIS3*	Obara *et al*., 2006
YOK219	SEY6210 *atg14*Δ::*LEU2 vps38*Δ::*HIS3*	Obara *et al*., 2006
KVY135	SEY6210 *vps30*Δ::*LEU2*	Kirisako *et al*., 2000
KVY135	SEY6210 *atg7*Δ::*HIS3*	Kirisako *et al*., 2000
BJ2168	*MATa leu2 trp1 ura3-52 pep4-3 prb1-1122 prc1-407*	Y.G.S.C

Y.G.S.C.: Yeast Genetic stock Center.

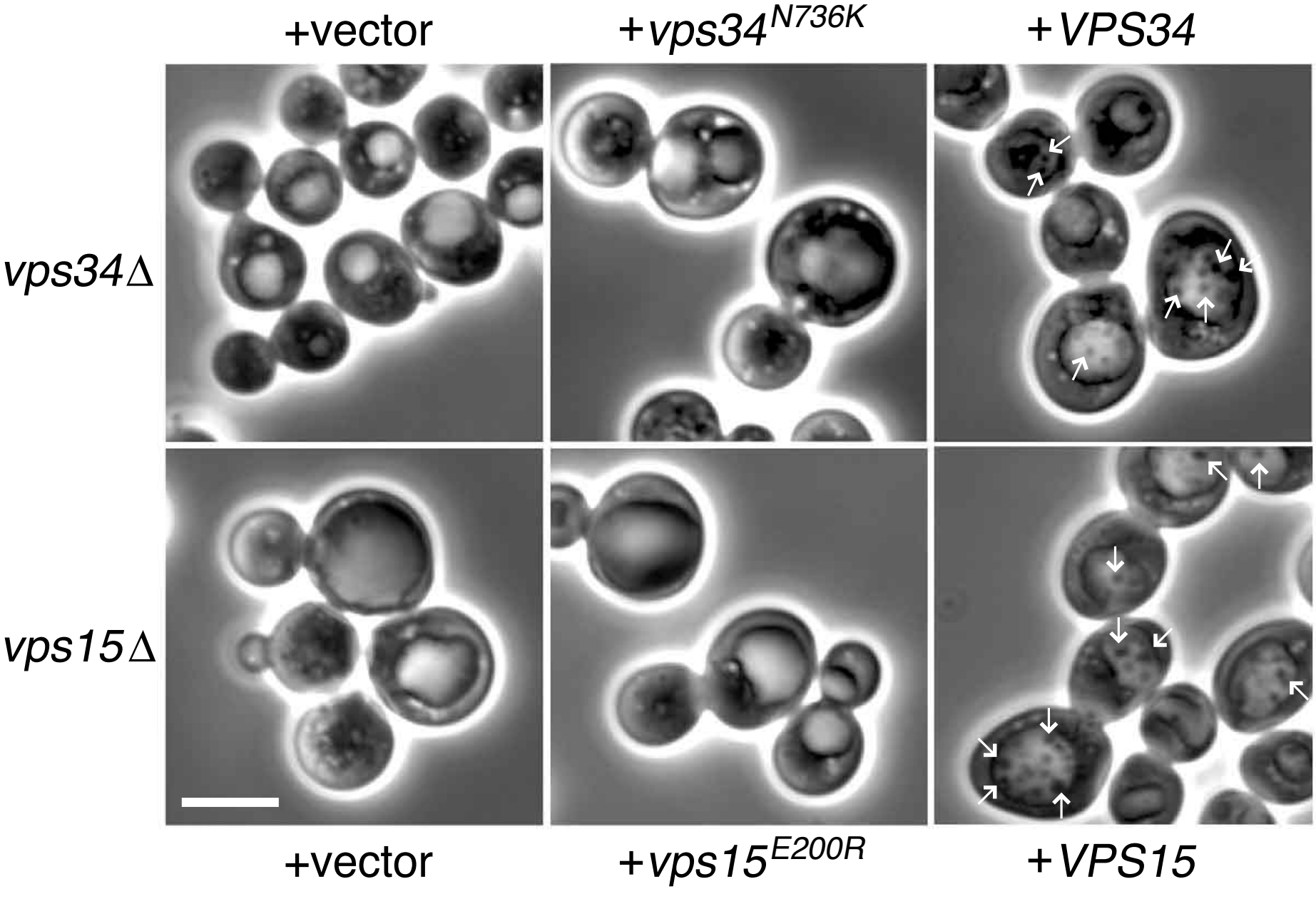
+vector
+vps34N736K
+VPS34
vps34Δ
vps15Δ
+vector
+vps15E200R
+VPS15

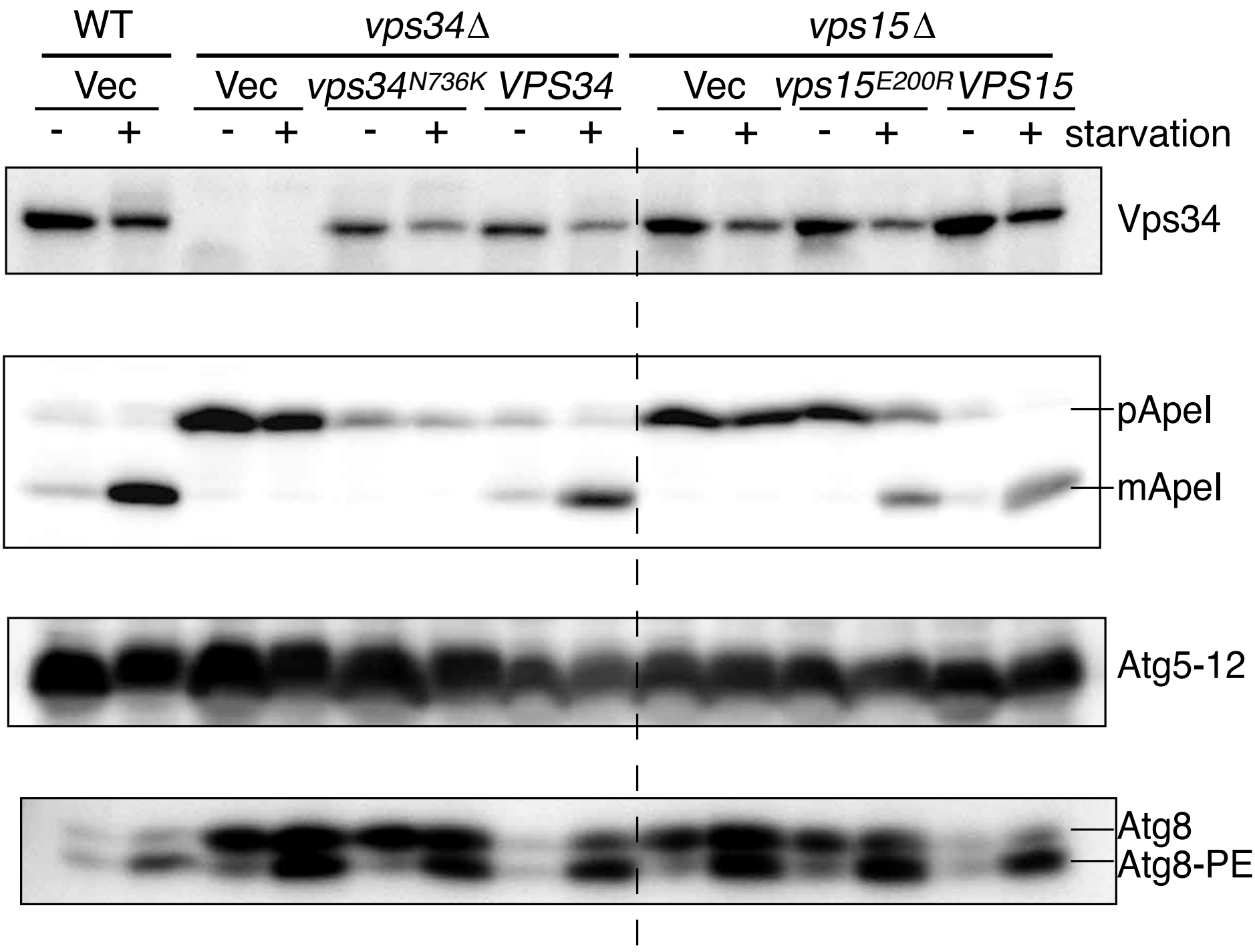
WT
vps34Δ
vps15Δ
Vec
Vec
vps34N736K
VPS34
Vec
vps15E200R
VPS15
- + - + - + - + - + - + starvation
Vps34
pApeI
mApeI
Atg5-12
Atg8
Atg8-PE

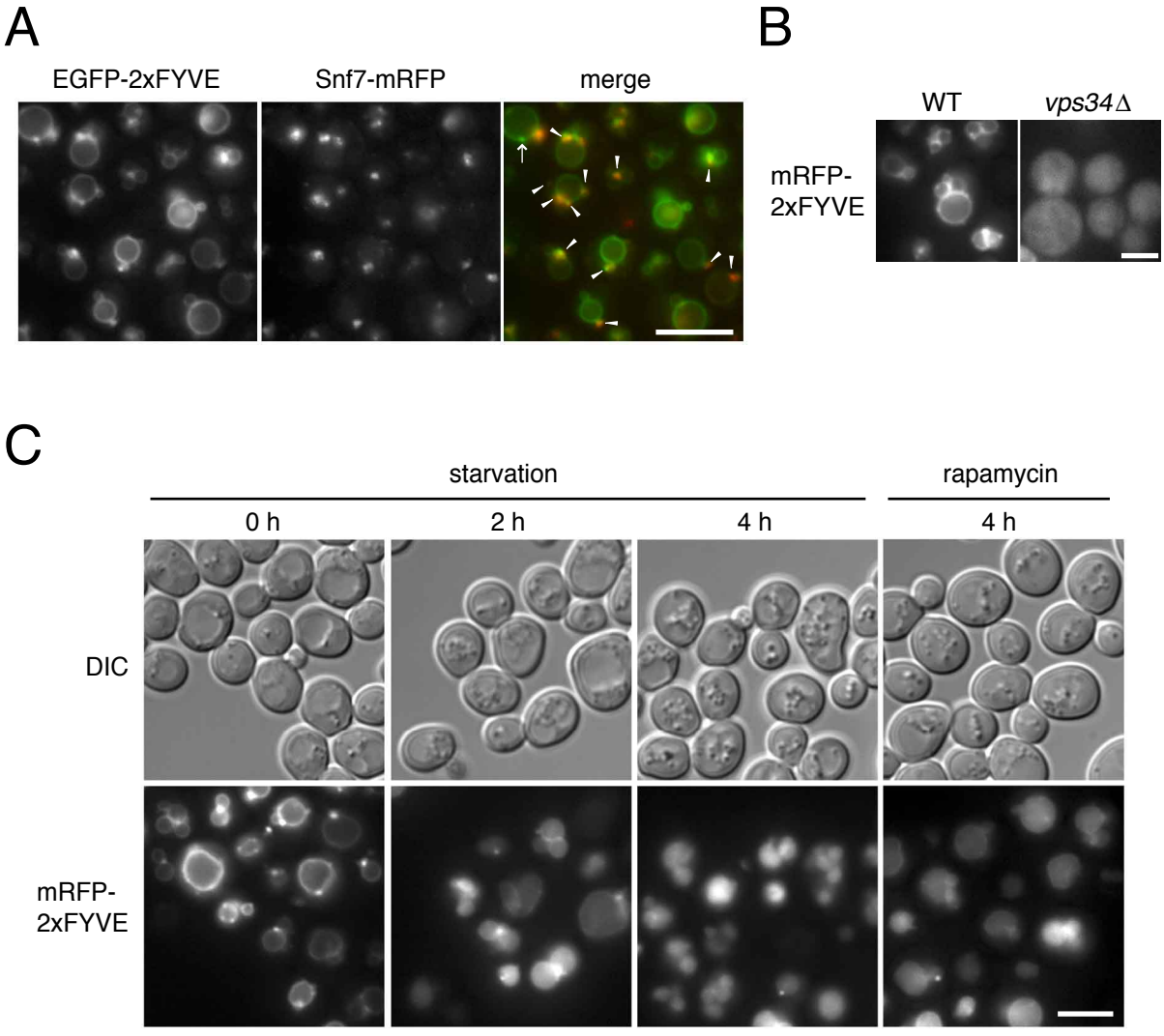
A
EGFP-2xFYVE
Snf7-mRFP
merge
B
WT
vps34Δ
mRFP-
2xFYVE
C
starvation
rapamycin
0 h
2 h
4 h
4 h
DIC
mRFP-
2xFYVE

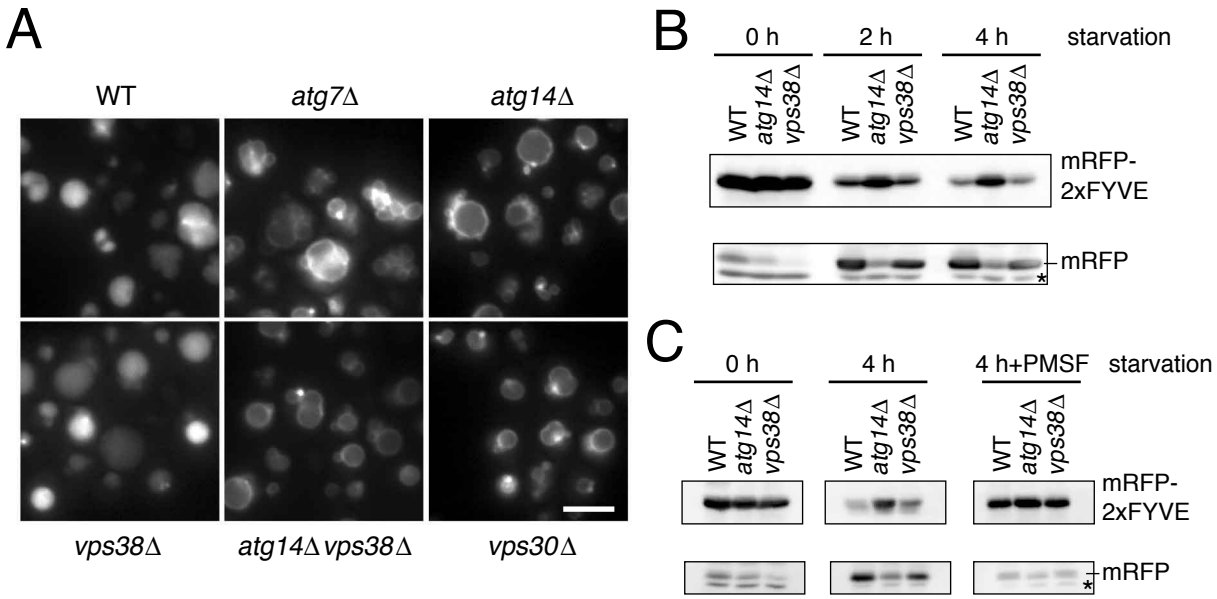
A
WT
atg7Δ
atg14Δ
vps38Δ
atg14Δ vps38Δ
vps30Δ
B
0 h
2 h
4 h
starvation
WT
atg14Δ
vps38Δ
mRFP-
2xFYVE
mRFP
*
C
0 h
4 h
4 h+PMSF
starvation
WT
atg14Δ
vps38Δ
mRFP-
2xFYVE
mRFP
*

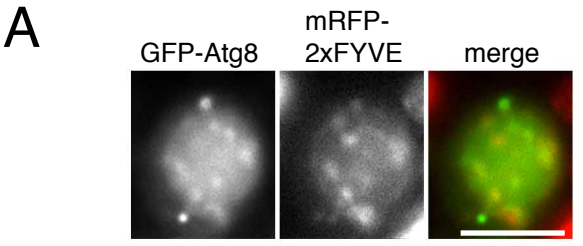
A
GFP-Atg8
mRFP-
2xFYVE
merge

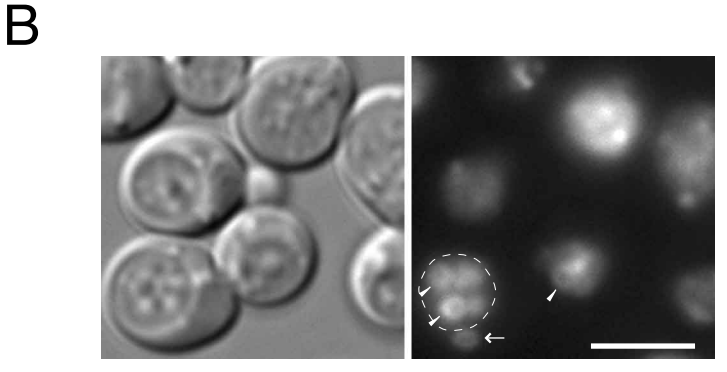
B

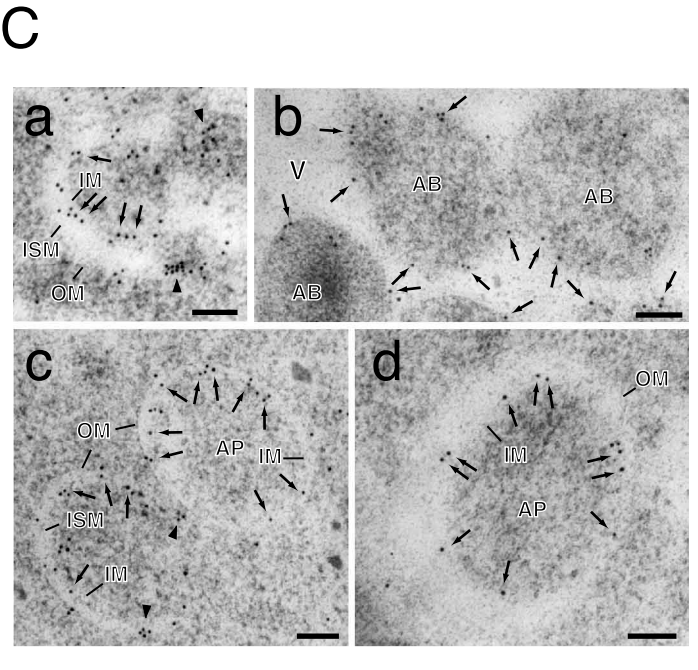
C
a
IM
ISM
OM
b
V
AB
AB
AB
c
OM
AP
IM
ISM
IM
d
OM
IM
AP